

Compounding formula approach to chromatin and active polymer dynamics

Takahiro Sakaue

Department of Physical Sciences, Aoyama Gakuin University,
5-10-1 Fuchinobe, Chuo-ku, Sagamihara, Japan*

Enrico Carlon

Soft matter and Biophysics, KU Leuven, Celestijnenlaan 200D, B-3001, Leuven, Belgium

Active polymers are ubiquitous in nature, and often kicked by persistent noises that break detailed balance. In order to capture the out-of-equilibrium dynamics of such active polymers, we propose a simple yet reliable analytical framework based on a *compounding formula*. Connecting polymeric dynamics to the isolated monomeric behavior via the notion of *tension propagation*, the formula allows us to clarify rich scaling scenarios alongside corresponding intuitive physical pictures. We demonstrate distinctive transient and steady-state scalings due to the non-Markovian nature of the active noise. Aside from a paradigmatic example of an active Rouse polymer, we expect the framework to be applicable to wide variety of spatially extended systems including more general polymers (crumpled globule, semiflexible polymers etc), fluctuation of growing interface, and an array of particles in single-file configuration.

Introduction – Chromatin, the complex of DNA and histone proteins found in living cells, provides a paradigmatic example of an active polymeric system whose dynamics have been intensively studied by experiments and theoretical modeling. Chromatin exhibits non-equilibrium dynamics due to the presence of various ATP-driven molecular motors as loop extruders, RNA polymerases or histone remodeling enzymes [1–5]. Chromatin dynamics is usually analyzed experimentally by tagging some specific sites with fluorophores, whose positions are then tracked over time [6–14]. The mean-squared displacement (MSD) of the tagged locus shows an anomalous dynamics, in many cases fitting the passive Rouse model behavior $\sim t^{1/2}$ but often showing complex crossovers [11] and sometimes superdiffusion $\sim t^\alpha$ (with $\alpha > 1$) which are likely signatures of underlying active processes dominating over thermal noise [2, 5]. Much of our knowledge about the active chromatin dynamics stems from the analysis of the active Rouse model (see below), which can be solved exactly [15–21], or numerical simulation of the related models [22–27]. Still, our current understanding lags behind the equilibrium counterpart largely due to the lack of clear-cut physical picture behind the rich non-equilibrium dynamics. The aim of this paper is to develop a scaling theory of the active Rouse model dynamics which will allow us to obtain a deeper understanding of the physical origin of the observed behavior. In addition, the scaling theory can be extended to cases which are not exactly solvable. The spirit is very much the same as in equilibrium Rouse model: from the analysis of such a model one develops scaling insights that can be used to infer, for instance, the effect of self-avoidance, which cannot be derived from exact calculations [28–32].

In the Rouse model the time evolution of $z(n, t)$ a cartesian component of the n^{th} monomer position is governed by the following Langevin equation

$$\gamma \frac{\partial z(n, t)}{\partial t} = k \frac{\partial^2 z(n, t)}{\partial n^2} + f(n, t) \quad (1)$$

where γ is the monomeric friction coefficient and k is the spring constant. We use a continuous description with n a real number which assumes both positive and negative values, as we consider an infinitely long polymer. Equation (1) represents the force balance in the overdamped limit with $k\partial_n^2 z(n, t)$ the elastic force on the n^{th} monomer due to the neighboring monomers and $f(n, t)$ all other forces, possibly including active ones. We will consider forces of stochastic origin $\langle f \rangle = 0$ and characterized by the correlator

$$\langle f(n, t)f(n', t') \rangle = Ag(|t - t'|)\delta(n - n') \quad (2)$$

with A measuring the noise strength. The thermal (passive) noise limit is $A = 2\gamma k_B T$ and $g(u) = \delta(u)$, but we will develop here an analysis valid for a generic function $g(u)$, which could contain an active and a passive component. Considering a long polymer and neglecting end terms effects, we build up the general solution from the propagator

$$G(n, t) = \left(\frac{\tau_0}{4\pi t} \right)^{1/2} \exp \left(-\frac{\tau_0}{4t} n^2 \right) \quad (3)$$

which solves (1) for $f = 0$, with the monomeric time scale defined as $\tau_0 = \gamma/k$. We recall that the normal mode approach to solve the Rouse model [28] typically applies to finite length chains with $0 \leq n \leq N$. In the equilibrium Rouse model the tagged monomer MSD shows a crossover from an anomalous ($\sim t^{1/2}$) to a regular ($\sim t$) diffusive behavior at the Rouse time scale $\tau_R \simeq \tau_0 N^2$. In our case ($N \gg 1$), we assume that the crossover to ordinary center of mass diffusion regime for times beyond the Rouse time τ_R exceeds any time scale of relevance for the system.

Tension propagation and compounding formula – The central result of this paper is the following compounding formula

$$\langle \Delta z^2(n, \tau) \rangle \simeq \frac{\langle \Delta z_i^2(\tau) \rangle}{m(\tau)} \quad (4)$$

where the symbol \simeq denotes a quasi-equality, i.e. it neglects multiplicative factor of order unity. The previous formula expresses the MSD of the n^{th} monomer

* sakaue@phys.aoyamna.ac.jp

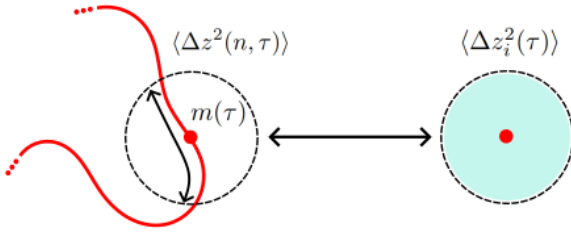


FIG. 1. The compounding formula (4) connects the MSD of a monomer of the chain (left) to that of an isolated monomer with an effective friction $m(\tau)\gamma$, with m the number of “dynamically connected monomers” (right).

[33] over a time scale τ as the ratio of the MSD of an isolated monomer $\langle \Delta z_i^2(\tau) \rangle$ with a factor $m(\tau)$ that accounts for the number of monomers which are “dynamically correlated” to the n^{th} monomer over a time scale τ , Fig. 1. The isolated monomer MSD can be obtained from the solution of (1) with $k = 0$ (thereby eliminating the chain connectivity), while $m(\tau)$ arises from mechanisms of tension propagation, i.e. the spreading of mechanical forces through the polymer chain. Tension propagation is central in the analysis of dynamical processes in polymers such as translocation [34–43], stretching [44, 45], folding and relaxation [46–48]. The factor $m(\tau)\gamma$ can be viewed as a timescale-dependent friction, which slows down the isolated monomer dynamics when $m(\tau)$ grows with τ . The interesting feature of Eq. (4) is that it disentangles the complex problem of the MSD of a monomer within a polymer chain into two contributions which are easier to rationalize, as we shall see from examples in which exact results and scaling arguments are presented.

Exact results: Transient and steady state - We are going to discuss next two different types of setups, as illustrated in Fig. 2. In the transient case the polymer is settled in thermal equilibrium and active noise is switched on at time s and the MSD is calculated from the differences in monomer positions between time s and t . In the steady state case, the active noise is switched on in a distant past, at a time $-T_\infty$, with T_∞ much larger than any other characteristic relaxation times of the system. Under these assumptions, the system at time s is in an active steady state. The MSD of the n^{th} monomer in the transient and steady state cases are different (for details see SI). Defining $\tau \equiv t - s$ we find for the transient case

$$\langle \Delta z^2(n, \tau) \rangle_t = \frac{2A}{\gamma^2} \sqrt{\frac{\tau_0}{4\pi}} \int_0^\tau du [\sqrt{2\tau - u} - \sqrt{u}] g(u) \quad (5)$$

while for the steady state the MSD is

$$\langle \Delta z^2(n, \tau) \rangle_s = \frac{2A}{\gamma^2} \sqrt{\frac{\tau_0}{4\pi}} \int_0^{T_\infty} du [\sqrt{\tau + u} - 2\sqrt{u} + \sqrt{|\tau - u|}] g(u) \quad (6)$$

The MSDs for transient and steady state are both expressed as integrals over the noise correlator $g(u)$, as defined in (2), with A the noise amplitude. The

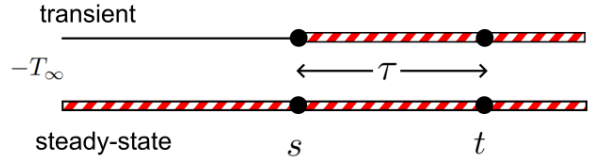


FIG. 2. The two cases considered. The red dashed area denotes the time interval during which the active noise is applied. In the transient case passive thermal white noise acts up to time $t = 0$. In the steady state case the initial condition is set at a time $-T_\infty$, with T_∞ longer than any characteristic times so that at time $t = 0$ an active steady state is reached. In both cases the MSD is calculated in the time interval $[0, \tau]$.

square root factors in (5) and (6) originate from integrating the Gaussian propagator $G(0, t) \sim t^{-1/2}$, Eq. (3), in different time intervals (see SI for details). In the transient case (5) the final MSD expression is an integral in the time domain $[0, \tau]$. In the steady state case, the integration is extended to the whole past history up to a time $-T_\infty$, reflecting the memory effects. In practice $g(u)$ is a decaying function of u therefore only a limited range of u contributes to the MSD. The isolated monomer MSD can be computed in a similar way and it is given by (see SI for details)

$$\langle \Delta z_i^2(\tau) \rangle = \frac{2A}{\gamma^2} \int_0^\tau du (\tau - u) g(u) \quad (7)$$

One does not distinguish in this case between steady state or transient dynamics. To complete the calculation of the terms entering in the compounding formula (4) we consider $m(\tau)$, the number of dynamically correlated monomers around the n^{th} monomer. The propagator (3) implies that any local perturbation applied at monomer n at time $t = 0$ grows with a variance linear in time $\sigma^2(t) = 2t/\tau_0$. The standard deviation gives then a measure of the number of monomers correlated to the perturbed monomer

$$m(\tau) \simeq \left(\frac{2\tau}{\tau_0} \right)^{1/2} \quad (8)$$

Figure 3 shows a test of the compounding formula (4) for the transient case and three different types of noise correlators $g(u)$. In all three cases we find excellent agreement between the n^{th} -monomer MSD (5), shown as solid lines, and the ratio of the isolated monomer MSD (7) and the number of dynamically correlated monomers (8), shown as dashed lines. The thin dotted lines are the asymptotic short and long time behavior. All noises show a universal $\sim \tau^{3/2}$ scaling at short times which crosses over to a regime $\sim \tau^{1/2}$ for the exponentially correlated noises (a, b). A different long time behavior is seen for the power-law correlated noise (c). The origin of these different scaling regimes are discussed in more details below.

Figure 4 analyzes the compounding formula for the steady state regime for the same three noises used in Fig. 3. The graphs show that Eq. (4) is verified throughout a broad range of time scales. In this case

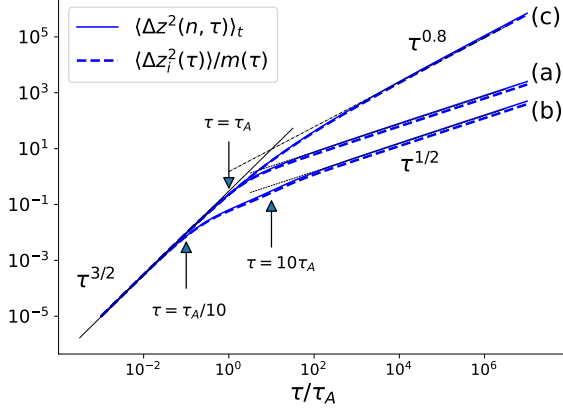


FIG. 3. Test of the validity of the compounding formula (4) for the transient case and three different noises: (a) $g(u) = e^{-u/\tau_A}$, (b) $g(u) = [100 e^{-10u/\tau_A} + e^{-u/(10\tau_A)}]/101$ and (c) $g(u) = 1/[1 + (u/\tau_A)^{0.7}]$. These are all normalized so that $g(0) = 1$. The solid lines are plots of Eq. (5), the tagged monomer MSD of a connected polymer. The dashed lines are plots of the ratio between Eqs. (7) and (8). The short time MSD scales as $\sim \tau^{3/2}$, while it asymptotically converges at long times to a $\sim \tau^{1/2}$ scaling in the exponentially correlated noise (a) and (b). The power-law correlated noise (c) generates a MSD with a different power-law behavior, see text.

the right hand side of the compounding formula we used

$$m(\tau) \simeq m_A + \left(\frac{2\tau}{\tau_0} \right)^{1/2} \quad (9)$$

for the number of dynamically correlated monomers, where $m_A \equiv (2\tau_A/\tau_0)^{1/2}$. This is because the active noise applied in the time interval $[-T_\infty, 0]$ generates an active steady state consisting of correlated domains of m_A monomers. Differently from the transient regime, the response to a perturbation at short times involves already the m_A monomers in the active correlated domains. At times $\tau \gg \tau_A$ the number of dynamically correlated monomers exceeds m_A and one recovers the same long time asymptotics as in the transient case, $m(\tau) \sim \tau^{1/2}$. Unlike the transient case, all cases exhibit a universal $\sim \tau^2$ scaling at short times. This is the contribution of the center-of-mass mode of the correlated dynamics of a segment of m_A monomers, which is the same ballistic scaling as that of an isolated monomer. As in the steady state regime m_A monomers are involved, the mobility is smaller than for an isolated monomer.

To gain more insight into the correlated domains, we report the result of the calculation of the displacement correlation between two distant monomers n_1 and $n_2 = n_1 + n$ over the time scale τ defined as $H(n, \tau) \equiv \langle \Delta z(n_1, \tau) \Delta z(n_2, \tau) \rangle_s$ (see SI). Note that $H(0, \tau) = \langle \Delta z^2(n_1, \tau) \rangle_s$ is the steady state MSD of the tagged monomer. For equilibrium dynamics we find (see SI for details) $H_{eq}(n, \tau) \sim \exp(-n^2 \tau_0/4\tau)$ for short times ($\tau \ll \tau_0 n^2$), while at long times ($\tau \gg \tau_0 n^2$) one recovers the anomalous dynamics behavior of the equilibrium Rouse model $H_{eq}(n, \tau) \sim \tau^{1/2}$.

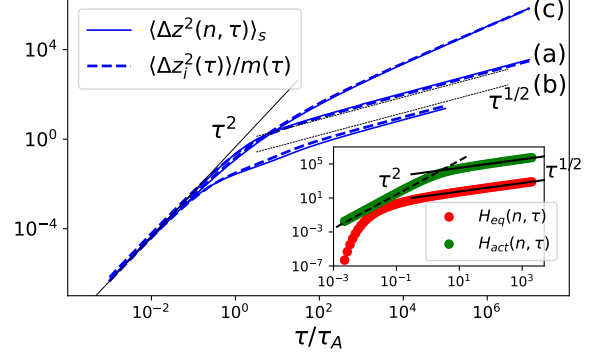


FIG. 4. Test of the compounding formula for the steady state case for the same three noises (a,b,c) as for the transient case of Fig. 3. The long time scale behavior is the same for steady state and transient case, but the short time scale is characterized by a $\text{MSD} \sim \tau^2$ in the former. See text for an explanation. Inset: plot of $H(\tau, n)$ vs. τ/τ_A and fixed n for equilibrium dynamics (red circles) and active steady state with exponentially correlated noise (green circles). The latter shows a short time power law ($\sim \tau^2$) behavior.

Hence, at a time scale τ , two distinct monomers perform correlated motion if they are within the range $|n_1 - n_2| \lesssim \sqrt{\tau/\tau_0}$ according to the tension propagation mechanism described by Eq. (8), see also [49]. In contrast, we find for the active steady-state at short scales as (see SI for details)

$$H_{act}(n, \tau) \approx \frac{A}{\gamma^2} \frac{e^{-n^2 \tau_0/4\tau_A}}{\sqrt{4\pi \tau_0}} \tau^2 \quad (\tau \ll \tau_A) \quad (10)$$

indicating that monomers within the domain $|n_1 - n_2| \lesssim \sqrt{\tau_A/\tau_0}$ perform correlated motion. Therefore the domain size is independent of the time scale, validating the picture of Eq. (9), i.e. that m_A monomers move collectively with their MSD given by $H_{act}(0, \tau)$.

Scaling: transient and steady-state – The results reported in Figs. 3 and 4 show that the compounding formula works well throughout a wide range of time scales. To understand the various regimes we use a scaling analysis. Let us consider first an isolated monomer, with MSD given in (7). At very short time scales, i.e. below a characteristic time $u \ll \tau_A$, the noise is $g(u) \approx 1$, which substituted in (7) gives

$$\langle \Delta z_i^2(\tau) \rangle \approx \frac{A}{\gamma^2} \tau^2 \quad (\tau \ll \tau_A) \quad (11)$$

At these time scales the random force preserves its magnitude (equal to \sqrt{A} , see (2)) and direction, leading to a uniform motion $z_i(\tau) \approx z_i(0) + v_0 \tau$ with velocity given by $v_0 = \sqrt{A}/\gamma$. This leads to (11). For the long-time behavior one should distinguish between exponentially decaying noise, as $g(u) = e^{-u/\tau_A}$, for which (7) yields (see SI for details)

$$\langle \Delta z_i^2(\tau) \rangle \approx \frac{A}{\gamma^2} \tau_A \tau \quad (\tau \gg \tau_A) \quad (12)$$

In this limit, one recovers the usual diffusion behavior, as the temporal correlation of the active force is

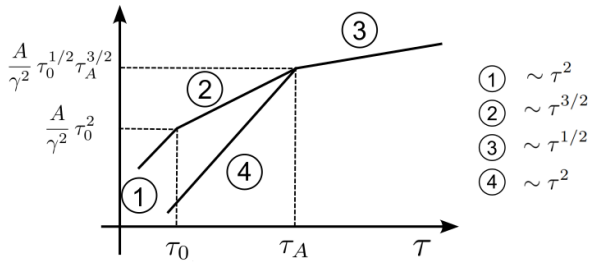


FIG. 5. Summary of the scaling prediction of the tagged monomer MSD in active Rouse polymer kicked by persistent noise (exponential correlation in this example). Time evolution follows a sequence of regimes 1 → 2 → 3 in the transient case, and 4 → 3 in the steady-state case.

lost due to its directional randomization. For a power-correlated noise decaying asymptotically as $g(u) \sim u^{-\alpha}$ ($\alpha < 1$), we find instead from the analysis of (7)

$$\langle \Delta z_i^2(\tau) \rangle \approx \tau^{2-\alpha} \quad (\tau \gg \tau_A) \quad (13)$$

with details reported in SI. Dividing now Eqs. (11), (12) and (13) by Eq. (8) one reproduces the short and long time behavior in Fig. 3 for the transient case. Using Eq. (9) instead of Eq. (8), one obtains all the results for the steady-state, see Fig. 4. Note that our compounding formula also includes the anomalous dynamics of a tagged monomer in the equilibrium Rouse model. In this case, Eqs. (8) and (9) coincide as $m_A = 0$, implying no distinction between transient and steady-state in scaling level (see SI for more quantitative discussion). An isolated monomer has an ordinary diffusive motion $\langle \Delta z_i^2(\tau) \rangle_{eq} = 2(k_B T / \gamma) \tau$, which divided by (8) gives the equilibrium Rouse result for the tagged monomer MSD [28]: $\sim \tau^{1/2}$.

Discussions and perspectives – The compounding formula (4), thus far tested for different type of noises and setups (transient vs steady state), is proven to be robust and to provide a solid theoretical framework through which one can analyze the dynamics of the active Rouse model. This allows us to resolve contradictory earlier works on the active Rouse model, which claimed MSD scaling either $\sim \tau^2$ [16, 20] or $\sim \tau^{3/2}$ [15, 18, 19, 50]. The main results are summarized in Fig. 5, which plots the various regimes of MSD for the steady state and transient dynamics. We restrict ourselves to showing the case of exponentially correlated noise $g(u) = \exp(-u/\tau_A)$, but this can be generalized to other cases as well. In this model, up to a time τ_A , the noise is persistent as the random force tend to point to the same direction leading to a direct ballistic motion. Beyond this time scale the effect of noise is similar to that of a delta-correlated thermal noise. The transient case of Fig. 5 is characterized by three distinct regimes, labeled as 1-2-3, and the steady state has a distinct scaling for $\tau < \tau_A$ (4). We summarize the scaling behaviors here. 1: Up to a monomer time scale τ_0 the monomer can be actually considered as free and under the effect of persistent noise the MSD scales as $\sim \tau^2$ [51]. 2: In the time interval $\tau_0 \leq \tau \leq \tau_A$ the effect of chain con-

nnectivity becomes apparent. The tension propagation mechanisms sets up and the number of dynamically connected monomers grows as in Eq. (8). This slows down the dynamics to an MSD scaling as $\sim \tau^{3/2}$. 3: Beyond $\tau \geq \tau_A$ the persistence effect of the active noise is lost and the scaling is as that of the thermal Rouse model $\sim \tau^{1/2}$. The tension propagation mechanism is still active in this regime and the MSD scaling is due to the ratio of ordinary diffusive motion $\sim \tau$ divided by $\sim \tau^{1/2}$, which is the tension propagation contribution of increasing dynamically correlated monomers, Eq. (4). 4: For the steady state case the MSD scales as τ^2 up to a time scale τ_A . The steady active noise generates correlated active domains, which respond collectively to the persistent noise.

Although our rigorous approach makes use of the linearity of the model and the resultant Gaussian form of the propagator, we expect that our scaling argument based on the compounding formula have much wider applicability. For instance, the self-avoidance or hydrodynamic interactions introduces the nonlinearity in the model, but these effects can be incorporated through the modified tension propagation scaling $m(\tau) \sim (\tau/\tau_0)^\beta$ [30, 32]. Yet another example is the so-called entanglement-free crumpled globule, for which $\beta = 3/5$ [50, 52]. In such cases, repeating our scaling argument with β exponent yields $\langle \Delta z(n, \tau)^2 \rangle_{eq} \simeq (k_B T / \gamma) \tau_0^\beta \tau^{1-\beta}$ for equilibrium dynamics. With active noise, we obtain

$$\langle \Delta z^2(n, \tau) \rangle \simeq \begin{cases} \frac{A}{\gamma^2} \tau_0^\beta \tau^{2-\beta} & (\text{transient, } \tau \ll \tau_A) \\ \frac{A}{\gamma^2} \left(\frac{\tau_0}{\tau_A} \right)^\beta \tau^2 & (\text{steady-state, } \tau \ll \tau_A) \\ \frac{A}{\gamma^2} \tau_0^\beta \tau_A \tau^{1-\beta} & (\tau \gg \tau_A) \end{cases}$$

with no distinction between transient and steady-state for longer time scale $\tau \gg \tau_A$, but $\tau_A \tau^{1-\beta}$ to be replaced by $\tau_A^\alpha \tau^{2-\alpha-\beta}$ if the noise decays slowly $g(u) \sim (u/\tau_A)^{-\alpha}$ ($\alpha < 1$) (see Fig. 3).

Equation (8) or its generalization with the exponent β is known to underlie various dynamical properties of unentangled polymer solutions [53, 54]. It is thus interesting to explore, for instance, the rheological consequence of the persistent active noise, where Eq. (9) supersedes. Our simple physical picture suggests the presence of the low frequency regime $\omega < \tau_A^{-1}$, where the solution may be viewed as the viscous solution composed of independent domains of size m_A , the viscosity of which is estimated as $\eta \sim A \tau_A^{2/3}$.

Lastly, there are several directions to extend the present study. Among others, the effect of inhomogeneous kicks, i.e., sparsity of the active noise source would be interesting in the context of chromatin dynamics, see refs [55–57] for related works. In addition, we point out the possible relevance to other systems than polymers. One example can be found in the problem of the growth of rough interfaces (see SI) [58–60]. It would be interesting to examine the validity of the compounding formula, for instance, in the growth model corresponding to the KPZ universality class with the persistent noise. Another system of interest is interacting particles in narrow channels, i.e., single-file diffusion [61]. We expect that our formalism applies to the dynamics of one-dimensional array

of active Brownian particles and also run-and-tumble particles[62].

Acknowledgments – We wish to express our gratitude to the late Carlo Vanderzande who introduced

us to the field of active polymers. T.S thanks J. Prost and G.V. Shivashankar for useful discussions. This work is supported by JSPS KAKENHI (Grant No. JP23H00369 and JP24K00602).

[1] S. C. Weber, A. J. Spakowitz, and J. A. Theriot, Proc. Natl. Acad. Sci. USA **109**, 7338 (2012).

[2] A. Javer *et al.*, Nat. Commun. **4**, 3003 (2013).

[3] D. Michieletto, D. Colò, D. Marenduzzo, and E. Orlandini, Phys. Rev. Lett. **123**, 228101 (2019).

[4] M. M. Tortora, H. Salari, and D. Jost, Curr. Op. Gen. Dev. **61**, 37 (2020).

[5] I. Eshghi, J. A. Eaton, and A. Zidovska, Phys. Rev. Lett. **126**, 228101 (2021).

[6] D. K. Sinha, B. Banerjee, S. Maharana, and G. Shivashankar, Biophys. J. **95**, 5432 (2008).

[7] I. Bronshtein *et al.*, Nat. Commun. **6**, 8044 (2015).

[8] T. J. Lampo, A. S. Kennard, and A. J. Spakowitz, Biophys. J. **110**, 338 (2016).

[9] N. Khanna, Y. Zhang, J. S. Lucas, O. K. Dudko, and C. Murre, Nat. Commun. **10**, 2771 (2019).

[10] S. S. Ashwin, K. Maeshima, and M. Sasai, Biophys. Rev. **12**, 461 (2020).

[11] A. K. Yesbolatova, R. Arai, T. Sakaue, and A. Kimura, Phys. Rev. Lett. **128**, 178101 (2022).

[12] M. Gabriele *et al.*, Science **376**, 496 (2022).

[13] V. I. P. Keizer *et al.*, Science **377**, 489 (2022).

[14] D. B. Bückner, H. Chen, L. Barinov, B. Zoller, and T. Gregor, Science **380**, 1357 (2023).

[15] H. Vandebroek and C. Vanderzande, Phys. Rev. E **92**, 060601 (2015).

[16] D. Osmanović and Y. Rabin, Soft Matter **13**, 963 (2017).

[17] N. Samanta and R. Chakrabarti, Journal of Physics A: Mathematical and Theoretical **49**, 195601 (2016).

[18] H. Vandebroek and C. Vanderzande, J. Stat. Phys. **167**, 14 (2017).

[19] S. Put, T. Sakaue, and C. Vanderzande, Phys. Rev. E **99**, 032421 (2019).

[20] R. G. Winkler and G. Gompper, J. Chem. Phys. **153**, 040901 (2020).

[21] K. Polovnikov and M. Kardar, arXiv preprint arXiv:2505.10943 (2025).

[22] A. Kaiser and H. Löwen, J. Chem. Phys. **141**, 044903 (2014).

[23] J. Shin, A. G. Cherstvy, W. K. Kim, and R. Metzler, New Journal of Physics **17**, 113008 (2015).

[24] L. Liu, G. Shi, D. Thirumalai, and C. Hyeon, PLoS. Comput. Biol. **14**, e1006617 (2018).

[25] J. Smrek, I. Chubak, C. Likos, and K. Kremer, Nat. Commun. **11**, 26 (2020).

[26] R. Das, T. Sakaue, G. Shivashankar, J. Prost, and T. Hiraiwa, eLife **11**, e79901 (2022).

[27] S. Brahmachari, T. Markovich, F. C. MacKintosh, and J. N. Onuchic, PRX Life **2**, 033003 (2024).

[28] M. Doi and S. Edwards, *The Theory of Polymer Dynamics* (Oxford University Press, Oxford, 1988).

[29] D. Panja, J. Stat. Mech. Theor. Exp. **2010**, P06011 (2010).

[30] T. Sakaue, Phys. Rev. E **87**, 040601 (2013).

[31] A. Amitai and D. Holcman, Phys. Rev. E **88**, 052604 (2013).

[32] T. Saito and T. Sakaue, Phys. Rev. E **92**, 012601 (2015).

[33] For simplicity we focus on a single cartesian component and refer to $\langle \Delta z^2 \rangle$ as the MSD. The full MSD for a 3D dynamics would comprise the contributions of the x and y components as well.

[34] T. Sakaue, Phys. Rev. E **76**, 021803 (2007).

[35] T. Sakaue, Phys. Rev. E **81**, 041808 (2010).

[36] P. Rowghanian and A. Y. Grosberg, The Journal of Physical Chemistry B **115**, 14127 (2011).

[37] T. Ikonen, A. Bhattacharya, T. Ala-Nissila, and W. Sung, Europhysics Letters **103**, 38001 (2013).

[38] H. W. de Haan, D. Sean, and G. W. Slater, Phys. Rev. E **98**, 022501 (2018).

[39] T. Saito and T. Sakaue, Phys. Rev. E **85**, 061803 (2012).

[40] J. Sarabadani, T. Ikonen, H. Mökkönen, T. Ala-Nissila, S. Carson, and M. Wanunu, Sci. Rep. **7**, 7423 (2017).

[41] J. Sarabadani, S. Buyukdagli, and T. Ala-Nissila, J. Phys. Condens. Matter. **32**, 385101 (2020).

[42] T. Sakaue, Polymers **8**, 424 (2016).

[43] A. Suma and C. Micheletti, Proc. Natl. Acad. Sci. U. S. A. **114**, E2991 (2017).

[44] T. Sakaue, T. Saito, and H. Wada, Phys. Rev. E **86**, 011804 (2012).

[45] P. Rowghanian and A. Y. Grosberg, Phys. Rev. E **86**, 011803 (2012).

[46] R. Frederickx, T. In't Veld, and E. Carlon, Phys. Rev. Lett. **112**, 198102 (2014).

[47] J.-C. Walter, M. Baiesi, E. Carlon, and H. Schiessel, Macromolecules **47**, 4840 (2014).

[48] T. Sakaue, J.-C. Walter, E. Carlon, and C. Vanderzande, Soft Matter **13**, 3174 (2017).

[49] N. Katayama and T. Sakaue, Soft Matter **21**, 5871 (2025).

[50] T. Sakaue and T. Saito, Soft Matter **13**, 81 (2017).

[51] We note that this regime is not observed in the plots of Fig. 3 as the analytical solution (5) is for a continuous model. In this $\tau \lesssim \tau_0$ regime, the monomer does not feel the connectivity with the rest of the chain and diffuses as a free monomer under a persistent noise.

[52] M. V. Tamm, L. I. Nazarov, A. A. Gavrilov, and A. V. Chertovich, Phys. Rev. Lett. **14**, 178102 (2015).

[53] P.-G. de Gennes, *Scaling Concepts in Polymer Physics* (Cornell University Press, 1979).

[54] M. Rubinstein and R. H. Colby, *Polymer Physics* (Oxford, 2003).

[55] S. Joo, X. Durang, O.-c. Lee, and J.-H. Jeon, Soft Matter **16**, 9188 (2020).

[56] H.-T. Han, S. Joo, T. Sakaue, and J.-H. Jeon, J. Chem. Phys. **159**, 024901 (2023).

[57] A. Goychuk, D. Kannan, A. K. Chakraborty, and M. Kardar, Proc. Natl. Acad. Sci. U. S. A. **120**, e2221726120 (2023).

[58] M. Kardar, G. Parisi, and Y.-C. Zhang, Phys. Rev. Lett. **56**, 889 (1986).

[59] A.-L. Barabási and H. E. Stanley, *Fractal concepts in surface growth* (Cambridge University Press, Cambridge, England, 1995).

[60] K. A. Takeuchi, Physica A **504**, 77 (2018).

[61] T. Ooshida, S. Goto, T. Matsumoto, and M. Otsuki, Biophys. Rev. Lett. **11**, 9 (2016).

[62] S. Paul, A. Dhar, and D. Chaudhuri, Soft Matter **20**, 8638 (2024).

SUPPLEMENTAL MATERIAL

This Supplemental Material is organized as follows. In Sec. I and II we present the calculations of the MSDs of an unconnected/isolated monomer and of a tagged monomer, respectively. The end results are given in Eq. (3) and Eqs. (17) for the steady-state, (21) for the transient case. These are Eqs. (5-7) of the main text. The calculations of the tagged monomer MSD are rather lengthy and the full details are given in Sec. II A. Section III reports the calculations of the quantity $H(n, \tau)$, which is the displacement correlation of two monomers n_1, n_2 with $|n_1 - n_2| = n$. Such quantity is plotted in the inset of Fig. 4. Finally, Section IV shows a summary of equilibrium dynamics, including the Rouse anomalous MSD dynamics $\sim \sqrt{\tau}$.

I. UNCONNECTED MONOMER DYNAMICS

An isolated monomer, unconnected with the rest of a polymer chain, moves via a random force $f(t)$ with autocorrelation given by

$$\langle f(t)f(t') \rangle = Ag(|t - t'|) \quad (1)$$

The cartesian coordinate position of the monomer is

$$z_i(\tau) = z_i(0) + \frac{1}{\gamma} \int_0^\tau dt f(t) \quad (2)$$

defining $\Delta z_i(\tau) \equiv z_i(\tau) - z_i(0)$, we find the mean-squared displacement

$$\langle \Delta z_i(\tau)^2 \rangle = \frac{2A}{\gamma^2} \int_0^\tau dt' \int_0^{t'} dt'' g(t' - t'') = \frac{2A}{\gamma^2} \int_0^\tau du g(u) \int_{u/2}^{\tau-u/2} dw = \boxed{\frac{2A}{\gamma^2} \int_0^\tau du (\tau - u) g(u)} \quad (3)$$

where we used the following change of variables $u \equiv t' - t''$ and $w = (t' + t'')/2$. This is Eq. (7) reported in the main text.

II. TAGGED MONOMER DYNAMICS: STEADY STATE AND TRANSIENT

The dynamics of $z(n, t)$, the position of the monomer n at time t is described by the following Langevin equation

$$\gamma \frac{\partial z(n, t)}{\partial t} = k \frac{\partial^2 z(n, t)}{\partial n^2} + f(n, t) \quad (4)$$

Its solution at time t , given an initial condition $z(n, s)$ at some earlier time $s < t$ can be written as

$$z(n, t; s) = \frac{1}{\gamma} \int dn' \int_s^t dt' G(n - n', t - t') f(n', t') + \int dn' G(n - n', t - s) z(n', s) \quad (5)$$

with $G(n, t)$ the Gaussian propagator defined as

$$G(n, t) = \sqrt{\frac{\tau_0}{4\pi t}} \exp\left(-\frac{\tau_0}{4t} n^2\right) \quad (6)$$

The integration in n' in (5) is extended over the whole real domain, corresponding to an infinitely long polymer. In the limit $t \rightarrow s$ the first integral in (5) vanishes and the second reduces to $z(n, s)$ as $\lim_{t \rightarrow s} G(n - n', t - s) = \delta(n - n')$. We are interested in the calculation of the displacement of the n -th monomer over a time interval $\tau \equiv t - s$, which is given by

$$\begin{aligned} \Delta z_n(s \rightarrow t; -T_\infty) &\equiv z(n, t; -T_\infty) - z(n, s; -T_\infty) \\ &= \frac{1}{\gamma} \int dn' \left[\int_{-T_\infty}^t dt' G(n - n', t - t') f(n', t') - \int_{-T_\infty}^s dt' G(n - n', s - t') f(n', t') \right] \end{aligned} \quad (7)$$

where we consider T_∞ sufficiently large and set $z(n, -T_\infty) = 0$, so that the last term in (5) vanishes. This initial condition does not influence the dynamics in the time interval $[s, t]$ if T_∞ is large enough. Adding and subtracting to (7) the quantity

$$\frac{1}{\gamma} \int dn' \int_{-T_\infty}^s dt' G(n - n', t - t') f(n', t') \quad (8)$$

we can rewrite the displacement as

$$\Delta z_n(s \rightarrow t; -T_\infty) = \mathcal{A}_n(\tau) + \mathcal{B}_n(\tau) \quad (9)$$

with

$$\mathcal{A}_n(\tau) \equiv \frac{1}{\gamma} \int dn' \int_s^t dt' G(n - n', t - t') f(n', t') \quad (10)$$

$$\mathcal{B}_n(\tau) \equiv \frac{1}{\gamma} \int dn' \int_{-T_\infty}^s dt' [G(n - n', t - t') - G(n - n', s - t')] f(n', t') \quad (11)$$

where $\tau = t - s$. The mean squared displacement is given by

$$\langle \Delta z_n^2 \rangle(s \rightarrow t; -T_\infty) = \langle \mathcal{A}_n(\tau)^2 \rangle + \langle \mathcal{B}_n(\tau)^2 \rangle + 2\langle \mathcal{A}_n(\tau) \mathcal{B}_n(\tau) \rangle \quad (12)$$

where the average $\langle \cdot \rangle$ is performed over the noise realizations. We find in the limit $T_\infty \rightarrow \infty$ (the details of the calculations are given in the last Section of this Supplemental)

$$\langle \mathcal{A}_n(\tau)^2 \rangle = \frac{A}{\gamma^2} \sqrt{\frac{\tau_0}{\pi}} \int_0^\tau du g(u) [\sqrt{2\tau - u} - \sqrt{u}] \quad (13)$$

$$\langle \mathcal{B}_n(\tau)^2 \rangle = \frac{A}{\gamma^2} \sqrt{\frac{\tau_0}{\pi}} \int_0^{+\infty} du g(u) [2\sqrt{u + \tau} - \sqrt{u + 2\tau} - \sqrt{u}] \quad (14)$$

$$\begin{aligned} 2\langle \mathcal{A}_n(\tau) \mathcal{B}_n(\tau) \rangle &= \frac{A}{\gamma^2} \sqrt{\frac{\tau_0}{\pi}} \left[\int_0^\tau du g(u) (\sqrt{2\tau + u} - \sqrt{2\tau - u} - \sqrt{\tau + u} + \sqrt{\tau - u}) + \right. \\ &\quad \left. \int_\tau^{+\infty} du g(u) (\sqrt{2\tau + u} - \sqrt{u} - \sqrt{\tau + u} + \sqrt{u - \tau}) \right] \end{aligned} \quad (15)$$

where we have defined $\tau \equiv t - s$ and used

$$\langle f(n, t) f(n', t') \rangle = A \delta(n - n') g(|t - t'|) \quad (16)$$

Summing up the three terms (13), (14) and (15) we find

$$\begin{aligned} \langle \Delta z_n^2(\tau) \rangle_s &= \langle \mathcal{A}_n(\tau)^2 \rangle + \langle \mathcal{B}_n(\tau)^2 \rangle + 2\langle \mathcal{A}_n(\tau) \mathcal{B}_n(\tau) \rangle \\ &= \boxed{\frac{A}{\gamma^2} \sqrt{\frac{\tau_0}{\pi}} \int_0^{+\infty} du g(u) (\sqrt{\tau + u} - 2\sqrt{u} + \sqrt{|\tau - u|})} \end{aligned} \quad (17)$$

which is the steady-state MSD expression Eq. (6) in the main text.

In the transient case we apply equilibrium dynamics during the whole process. At time $t > s$, additional active noise term is turned on. The stochastic noise is therefore

$$f(n, t) = \eta(n, t) + \theta(t - s) f_a(n, t) \quad (18)$$

with $\eta(n, t)$ the equilibrium component

$$\langle \eta(n, t) \eta(n', t') \rangle = A_{th} \delta(n - n') g_{th}(t - t') \quad (19)$$

where $A_{th} = 2\gamma k_B T$, $g_{th}(u) = \delta(u)$ and $\theta(t)$ the Heaviside step function and $f_a(t)$ the active component

$$\langle f_a(n, t) f_a(n, t') \rangle = A \delta(n - n') g(|t - t'|) \quad (20)$$

We moreover assume that η and f_a are uncorrelated. From their definitions, \mathcal{A}_n has both thermal and active components, while \mathcal{B}_n has only thermal component. The mean-square displacement in this transient case is given by

$$\begin{aligned} \langle \Delta z_n^2(\tau) \rangle_t &= \langle \mathcal{A}_n(\tau)^2 \rangle + \langle \mathcal{A}_n(\tau)^2 \rangle_{eq} + \langle \mathcal{B}_n(\tau)^2 \rangle_{eq} = \frac{A}{\gamma^2} \sqrt{\frac{\tau_0}{\pi}} \int_0^\tau du g(u) [\sqrt{2\tau - u} - \sqrt{u}] + \frac{2k_B T}{\gamma} \sqrt{\frac{\tau_0 \tau}{\pi}} \\ &\approx \boxed{\frac{A}{\gamma^2} \sqrt{\frac{\tau_0}{\pi}} \int_0^\tau du g(u) [\sqrt{2\tau - u} - \sqrt{u}]} \end{aligned} \quad (21)$$

where we have assumed that the active component dominates over the thermal one. In this limit the previous equation reproduces Eq. (5) of the main text. Note the absence of the cross term $\langle \mathcal{A}_n \mathcal{B}_n \rangle$ in the transient set-up, where $\mathcal{B}_n(\tau)$ has only the equilibrium component; the cross term exists only for the noise with temporal correlation, see definition of these terms in Eq.(10) and (11), thus, identically vanishes for white noise. The thermal contribution to the MSD is the usual $\sim \sqrt{\tau}$ contribution which is the familiar tagged monomer dynamics of the equilibrium Rouse model.

A. Details of the calculations of $\langle \mathcal{A}_n^2 \rangle$, $\langle \mathcal{B}^2 \rangle$ and $\langle \mathcal{A}_n \mathcal{B}_n \rangle$

To derive the final expressions we used (16) and

$$\int dn' G(n - n', \tau) G(n' - n'', \tau') = G(n - n'', \tau + \tau') \quad (22)$$

which follows from elementary properties of the Gaussian propagator (6).

1. Calculation of $\langle \mathcal{A}_n^2 \rangle$

From the definition of $\mathcal{A}_n(\tau)$, see Eq. (10), we have

$$\begin{aligned} \langle \mathcal{A}_n(\tau)^2 \rangle &= \frac{1}{\gamma^2} \int dn' dn'' \int_s^t dt' dt'' G(n - n', t - t') G(n - n'', t - t'') \langle f(n', t') f(n'', t'') \rangle \\ &= \frac{A}{\gamma^2} \int_s^t dt' dt'' g(|t' - t''|) \int dn' G(n - n', t - t') G(n - n'', t - t'') \\ &= \frac{2A}{\gamma^2} \int_s^t dt' \int_s^{t'} dt'' g(t' - t'') G(0, 2t - t' - t'') \end{aligned} \quad (23)$$

where we used (22). With the following change of variables $u \equiv t' - t''$ and $w = 2(t - t')$ we can rewrite the integration domain as

$$\begin{aligned} \langle \mathcal{A}_n(\tau)^2 \rangle &= \frac{A}{\gamma^2} \int_0^\tau du g(u) \int_0^{2(\tau-u)} dw G(0, u + w) = \frac{A}{\gamma^2} \sqrt{\frac{\tau_0}{4\pi}} \int_0^\tau du g(u) \int_0^{2(\tau-u)} \frac{dw}{\sqrt{u+w}} \\ &= \frac{A}{\gamma^2} \sqrt{\frac{\tau_0}{\pi}} \int_0^\tau du g(u) (\sqrt{2\tau-u} - \sqrt{u}) \end{aligned} \quad (24)$$

with $\tau \equiv t - s$. This equation is (13) also reported as Eq. (5) in the main text.

2. Calculation of $\langle \mathcal{B}_n^2 \rangle$

We use the similar variable transformation as for the calculation of $\langle \mathcal{A}_n^2 \rangle$, where we set the argument in each G term to be $u + w$;

$$\langle \mathcal{B}_n(\tau)^2 \rangle = \frac{A}{\gamma^2} \int_0^{s+T_\infty} du g(u) \left[\int_{2\tau}^{2(\tau+(T_\infty+s)-u)} dw - 2 \int_\tau^{\tau+2(T_\infty+s-u)} dw + \int_0^{2(T_\infty+s-u)} dw \right] G(0, u + w)$$

where we employed a short-handed notation for the integral: $[\int_a^b dw + \int_c^d dw]G(w) \equiv \int_a^b dw G(w) + \int_c^d dw G(w)$. The integration range for w in the above equation can be arranged as

$$\begin{aligned} &\left[\int_{2\tau}^{2(\tau+(T_\infty+s)-u)} dw - 2 \int_\tau^{\tau+2(T_\infty+s-u)} dw + \int_0^{2(T_\infty+s-u)} dw \right] G(0, u + w) \\ &= \left[\int_0^\tau dw - \int_\tau^{2\tau} dw \right] G(0, u + w) - \left[\int_{2(T_\infty+s-u)}^{2(T_\infty+s-u)+\tau} dw - \int_{2(T_\infty+s-u)+\tau}^{2(T_\infty+s-u)+2\tau} dw \right] G(0, u + w) \\ &\stackrel{T_\infty \rightarrow +\infty}{=} \left[\int_0^\tau dw - \int_\tau^{2\tau} dw \right] G(0, u + w) \end{aligned} \quad (25)$$

where in the last line we took the limit $T_\infty \rightarrow +\infty$, which leads to the vanishing contribution from the last term. Substituting the form of $G(0, u)$, we find

$$\begin{aligned} \langle \mathcal{B}_n(\tau)^2 \rangle &\stackrel{T_\infty \rightarrow +\infty}{=} \frac{A}{\gamma^2} \sqrt{\frac{\tau_0}{4\pi}} \int_0^{+\infty} du g(u) \left[\int_0^\tau dw - \int_\tau^{2\tau} dw \right] \frac{1}{\sqrt{u+w}} \\ &= \frac{A}{\gamma^2} \sqrt{\frac{\tau_0}{\pi}} \int_0^{+\infty} du g(u) (2\sqrt{\tau+u} - \sqrt{2\tau+u} - \sqrt{u}) \end{aligned} \quad (26)$$

which is the result given in (14).

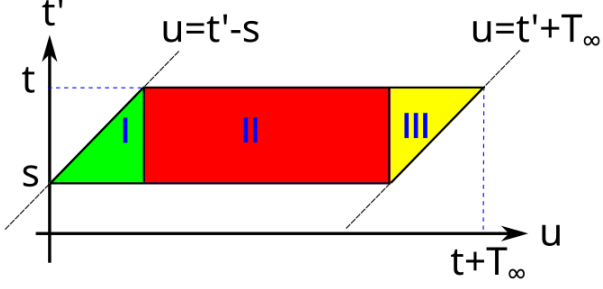


FIG. 6. Integration domain in the calculation of $\langle \mathcal{A}\mathcal{B} \rangle$ as function of the variables $u \equiv t' - t''$ and t' .

3. Calculation of $\langle \mathcal{A}_n \mathcal{B}_n \rangle$

From the definition of $\mathcal{A}_n(\tau), \mathcal{B}_n(\tau)$, see Eqs. (10), (11), we have

$$\begin{aligned} 2\langle \mathcal{A}_n(\tau) \mathcal{B}_n(\tau) \rangle &= \frac{2}{\gamma^2} \int dn' dn'' \int_s^t dt' \int_{-T_\infty}^s dt'' G(n - n', t - t') [G(n - n'', t - t'') - G(n - n'', s - t'')] \\ &\quad \langle f(n', t') f(n'', t'') \rangle = \frac{2A}{\gamma^2} \int_s^t dt' \int_{-T_\infty}^s dt'' g(t' - t'') [G(0, 2t - t' - t'') - G(0, s + t - t' - t'')] \end{aligned} \quad (27)$$

To proceed further we perform a change of variables defining $u \equiv t' - t''$ and using u and t' as integration variables. The integration domain is then $s \leq t' \leq t$ and $t' - s \leq u \leq t' + T_\infty$, which is shown in Fig. 6. We split this domain in three parts I, II and III, see Fig. 6, and proceed with integrating over each domain. Again, setting the argument in the G term to be $u + w$, we continue the calculation to find

$$\begin{aligned} 2\langle \mathcal{A}_n(\tau) \mathcal{B}_n(\tau) \rangle_I &= \frac{2A}{\gamma^2} \int_0^{t-s} du g(u) \int_s^{u+s} dt' [G(0, 2t + u - 2t') - G(0, s + t + u - 2t')] \\ &= \frac{A}{\gamma^2} \int_0^\tau du g(u) \left[\int_{2(\tau-u)}^{2\tau} dw - \int_{\tau-2u}^\tau dw \right] G(0, u + w) \end{aligned} \quad (28)$$

$$= \frac{A}{\gamma^2} \sqrt{\frac{\tau_0}{\pi}} \int_0^\tau du g(u) (\sqrt{2\tau + u} - \sqrt{2\tau - u} - \sqrt{\tau + u} + \sqrt{\tau - u}) \quad (29)$$

$$\begin{aligned} 2\langle \mathcal{A}_n(\tau) \mathcal{B}_n(\tau) \rangle_{II} &= \frac{2A}{\gamma^2} \int_{t-s}^{s+T_\infty} du g(u) \int_s^t dt' [G(0, 2t + u - 2t') - G(0, s + t + u - 2t')] \\ &= \frac{A}{\gamma^2} \int_\tau^{s+T_\infty} du g(u) \left[\int_0^{2\tau} dw - \int_{-\tau}^\tau dw \right] G(0, u + w) \end{aligned} \quad (30)$$

$$\stackrel{T_\infty \rightarrow +\infty}{=} \frac{A}{\gamma^2} \sqrt{\frac{\tau_0}{\pi}} \int_\tau^{+\infty} du g(u) (\sqrt{2\tau + u} - \sqrt{u} - \sqrt{\tau + u} + \sqrt{\tau - u}) \quad (31)$$

Finally $\langle \mathcal{A}_n(\tau) \mathcal{B}_n(\tau) \rangle_{III}$ vanishes in the limit $T_\infty \rightarrow \infty$. Summing up (29) and (31) one arrives at (15).

III. DISPLACEMENT CORRELATION $H(n, \tau)$

The correlation in displacement of two monomers n apart along the chain during the time scale τ can be quantified by the following correlation function;

$$H(n, \tau) \equiv \langle \Delta z_{n_1}(s \rightarrow t; -T_\infty) \Delta z_{n_2}(s \rightarrow t; -T_\infty) \rangle \quad (32)$$

where $n = |n_1 - n_2|$. We note that $H(0, \tau) = \langle \Delta z_{n_1}^2(s \rightarrow t; -T_\infty) \rangle$, which is the tagged monomer steady-state MSD. The translational invariance along the chain, valid for a long chain, and the time-translational invariance in the steady-state $T_\infty \rightarrow \infty$ implies that the correlation depends only on the separation n and $\tau = t - s$. Using the decomposition (9), the displacement correlation function can be written as

$$H(n, \tau) = \langle \mathcal{A}_n(\tau) \mathcal{A}_0(\tau) \rangle + 2\langle \mathcal{A}_n(\tau) \mathcal{B}_0(\tau) \rangle + \langle \mathcal{B}_n(\tau) \mathcal{B}_0(\tau) \rangle \quad (33)$$

where we have used $\langle \mathcal{A}_n(\tau) \mathcal{B}_0(\tau) \rangle = \langle \mathcal{B}_n(\tau) \mathcal{A}_0(\tau) \rangle$. To calculate these quantities, we can follow essentially the same step detailed above in the calculation of the mean square displacement. Indeed, with the replacement $G(0, u + w) \rightarrow G(n, u + w)$ in Eqs. (24), (25), (28), (30), we find

$$\langle \mathcal{A}_n(\tau) \mathcal{A}_0(\tau) \rangle = \frac{A}{\gamma^2} \int_0^\tau du g(u) \int_0^{2(\tau-u)} dw G(n, u + w) \quad (34)$$

$$\langle \mathcal{B}_n(\tau) \mathcal{B}_0(\tau) \rangle = \frac{A}{\gamma^2} \int_0^{+\infty} du g(u) \left[\int_0^\tau dw - \int_\tau^{2\tau} dw \right] G(n, u + w) \quad (35)$$

$$\begin{aligned} 2\langle \mathcal{A}_n(\tau) \mathcal{B}_0(\tau) \rangle &= \frac{A}{\gamma^2} \int_0^\tau du g(u) \left[\int_{2(\tau-u)}^{2\tau} dw - \int_{\tau-2u}^\tau dw \right] G(n, u + w) \\ &\quad + \frac{A}{\gamma^2} \int_\tau^{+\infty} du g(u) \left[\int_0^{2\tau} dw - \int_{-\tau}^\tau dw \right] G(n, u + w) \end{aligned} \quad (36)$$

Breaking the integration range of u in $\langle \mathcal{B}_n(\tau) \mathcal{B}_0(\tau) \rangle$ as $\int_0^{+\infty} du = \int_0^\tau du + \int_\tau^{+\infty} du$, we can write and arrange $H(n, \tau)$ as

$$\begin{aligned} H(n, \tau) &= \frac{A}{\gamma^2} \int_0^\tau du g(u) \left[\int_0^{2(\tau-u)} dw + \int_{2(\tau-u)}^{2\tau} dw - \int_{\tau-2u}^\tau dw + \int_0^\tau dw - \int_\tau^{2\tau} dw \right] G(n, u + w) \\ &\quad + \frac{A}{\gamma^2} \int_\tau^{+\infty} du g(u) \left[\int_0^\tau dw - \int_\tau^{2\tau} dw + \int_0^{2\tau} dw - \int_{-\tau}^\tau dw \right] G(n, u + w) \\ &= \frac{A}{\gamma^2} \int_0^\tau du g(u) \left[\int_0^\tau dw + \int_0^{\tau-2u} dw \right] G(n, u + w) + \frac{A}{\gamma^2} \int_\tau^{+\infty} du g(u) \left[\int_0^\tau dw - \int_{-\tau}^0 dw \right] G(n, u + w) \end{aligned} \quad (37)$$

Performing the integral over w , we obtain

$$H(n, \tau) = \frac{A}{\gamma^2} \left\{ \int_0^\tau du g(u) [F_n(\tau + u) - 2F_n(u) + F_n(\tau - u)] + \int_\tau^{+\infty} du g(u) [F_n(\tau + u) - 2F_n(u) + F_n(u - \tau)] \right\} \quad (38)$$

where we have defined $F_n(u) \equiv \int_0^u dw G(n, w)$. It is convenient to rewrite $F_n(\tau)$, using some variable transformations and integration by parts, as follows

$$\begin{aligned} F_n(\tau) &= \int_0^\tau \sqrt{\frac{\tau_0}{4\pi w}} e^{-\frac{n^2 \tau_0}{4w}} dw = \frac{n\tau_0}{4\sqrt{\pi}} \int_{\alpha^2(\tau)}^{+\infty} z^{-3/2} e^{-z} dz = \frac{n\tau_0}{2} \left[\frac{e^{-\alpha^2(\tau)}}{\sqrt{\pi}\alpha(\tau)} - \frac{2}{\sqrt{\pi}} \int_{\alpha(\tau)}^{+\infty} e^{-x^2} dx \right] \\ &= \frac{n\tau_0}{2} \left\{ \frac{e^{-\alpha^2(\tau)}}{\sqrt{\pi}\alpha(\tau)} - \text{Erfc}[\alpha(\tau)] \right\} \end{aligned} \quad (39)$$

where we defined $\alpha(\tau) \equiv \frac{n}{2} \sqrt{\frac{\tau_0}{\tau}}$ and with $\text{Erfc}(x)$ the complementary error function.

A. Equilibrium dynamics

We note that for the white noise $g(u) \sim \delta(u)$ and the second term in (38) identically vanishes. The first term gives (recall that $A = 2\gamma k_B T$ in equilibrium)

$$H_{eq}(n, \tau) = \frac{2k_B T}{\gamma} F_n(\tau) \quad (40)$$

The short and long time scale behavior can be derived from (39). At short times and fixed n the leading behavior is

$$H_{eq}(n, \tau) = \frac{2k_B T}{\gamma} F_n(\tau) \sim \tau^{3/2} e^{-\frac{n^2 \tau_0}{4\tau}} \quad \left(\tau \ll \frac{n^2 \tau_0}{2} \right) \quad (41)$$

where we used the asymptotic expansion of $\text{Erfc}(x)$ for large x , which is $\text{Erfc}(x) \approx (x\sqrt{\pi})^{-1} e^{-x^2} [1 - 1/(2x^2) + \dots]$. For long times $\alpha(\tau) \rightarrow 0$ in Eq. (39) therefore

$$H_{eq}(n, \tau) \approx \frac{k_B T \tau_0}{\gamma} \left[\sqrt{\frac{4\tau}{\pi \tau_0}} - n \right] \quad \left(\tau \gg \frac{n^2 \tau_0}{2} \right) \quad (42)$$

These results show that while two distal monomers on the chain are uncorrelated in their motion on short time scale, they start to move together on longer time scale [49]. The crossover time τ_n for two monomers with their separation n is given by $m(\tau_n) \simeq n$, where $m(\tau)$ is determined by the dynamics of tension propagation, see Eq.(8) in the main text.

B. Active dynamics

We now calculate $H(n, \tau)$ for a steady-state polymer kicked by persistent active noise with characteristic time τ_A ; the correlation can be exponential $g(u) = e^{-u/\tau_A}$ or more slowly decaying $g(u) = (1 + (u/\tau_A)^\alpha)^{-1}$ with $\alpha < 1$. In particular, we are interested in the short time-scale regime $\tau \ll \tau_A$. In this case, $g(u) \simeq 1$, hence, Eq.(38) is approximated as

$$\begin{aligned} H(n, \tau) &\simeq \frac{A}{\gamma^2} \int_0^\tau du [F_n(\tau + u) - F_n(u)] + \frac{A}{\gamma^2} \int_\tau^{\tau_A} du [F_n(\tau + u) - 2F_n(u) + F_n(-\tau + u)] \\ &= \frac{A}{\gamma^2} [E_n(\tau_A + \tau) - 2E_n(\tau_A) + E_n(\tau_A - \tau)] \simeq \frac{A}{\gamma^2} G(n, \tau_A) \tau^2 \end{aligned} \quad (43)$$

which is Eq. (10) of the main text, being $G(n, t)$ the Gaussian propagator. In the first line of (43), the relation $\int_0^\tau du F_n(\tau - u) = \int_0^\tau du F_n(u)$ is used inside the first integrand, and we have defined in the second line $E_n(u) \equiv \int_0^u dw F_n(w)$. The final expression is obtained by expansion up to second order around $u = \tau_A$ (recall $G(n, \tau_A) = \frac{\partial^2}{\partial u^2} E_n(u)|_{u=\tau_A}$), which is justified in the condition of interest $\tau \ll \tau_A$. The physical interpretation of the above result is the following. From the form of Gaussian propagator, $G(n, \tau_A) \ll 1$ for $n \gtrsim m_A = (2\tau_A/\tau_0)^{1/2}$. This number m_A , introduced in Eq. (9) in the main text, signifies the size of domain for the cooperative motion, which is independent of time scale in the steady-state maintained by the correlated active noise in the time-scale shorter than the noise decorrelation time.

In the transient case, the active noise is switched on at time s at which polymer assumes its equilibrium configuration. The noise is thus given by Eq. (18), hence, \mathcal{B}_n has only the equilibrium component, while \mathcal{A}_n has both the equilibrium and the active components. The contribution to the displacement correlation from the equilibrium component is given by Eq. (40). The active contribution is simply given by Eq. (34), which we can integrate over w and u with assuming $g(u) \simeq 1$, then, rewrite it as

$$H(n, \tau) = \frac{A}{\gamma^2} [E_n(2\tau) - 2E_n(\tau)] \quad (\text{active component in transient case}) \quad (44)$$

The displacement correlation function in transient case is the sum of Eqs. (40) and (44). In stark contrast to Eq. (43) for the active steady-state, where the spatial correlation is governed by $G(n, \tau_A)$, thus, no dependence on the time scale τ , we find τ -dependence in the transient case (recall $F_n(\tau), E_n(\tau)$ are obtained from $G(n, \tau)$ by integration). To summarize, for a given time scale τ , we can define the size $m(\tau) = (2\tau/\tau_0)^{1/2}$, i.e., Eq.(8) in the main text such that $H_{eq}(n, \tau)$ vanishes for $n \gtrsim m(\tau)$. The same property, i.e., the vanishing correlation for $n \gtrsim m(\tau)$ applies to the active contribution in transient case given in Eq. (44).

Finally, we comment that the equilibrium component is always present, but in our analysis in steady-state, we have neglected it by assuming that the active noise contribution dominates over the thermal contribution. We also note that in the special case $n = 0$, the displacement correlation $H(n, \tau)$ coincides to MSD, so the above expressions on $H(n, \tau)$ can be reduced to all the results in earlier sections in this limit.

IV. EQUILIBRIUM DYNAMICS: TRANSIENT VS. STEADY-STATE

For completeness, here we summarize the results for the equilibrium dynamics. Using Eqs. (12), (13), (14) and $A_{th} = 2\gamma k_B T$, $g_{th}(u) = \delta(u)$ (hence no cross term $\langle \mathcal{A}_n \mathcal{B}_n \rangle = 0$), we obtain the mean square displacement

$$\langle \Delta z_n(\tau)^2 \rangle = \frac{2k_B T}{\gamma} \sqrt{\frac{\tau_0}{\pi}} \tau^{1/2} \quad (45)$$

The same result is obtained from Eq. (40) by setting $n = 0$.

In the polymer problem, the thermal noise is assumed to be always present. For this reason, it would make no sense to distinguish the steady-state and transient scenarios in equilibrium, i.e., passive systems without active noise. So the above result, not only the well-known sub-diffusion scaling with exponent 1/2, but also its numerical prefactor, is generic for a Rouse polymer in thermal equilibrium. However, there would be other systems, where the distinction between two scenarios is meaningful. As an example, let us consider the interface that grows by random deposition of particles. Upon falling on the top of the interface, deposited particles are allowed to relax to the lowest height neighboring site. In the continuum limit, this process is described by

Eq. (1) in the main text, in this context, called Edwards-Wilkinson equation, where $z(n, t)$ represents the height of the interface on the one-dimensional substrate position n at time t and k plays the role of surface tension. The noise is usually assumed to be uncorrelated white noise, see Eq. (19). The model is thus equivalent to the equilibrium (passive) Rouse dynamics.

In the steady-state scenario in equilibrium dynamics, the interface is aged ($T_\infty \rightarrow \infty$) and settled in its steady-state in the presence of the uncorrelated white noise, and we monitor the height increment during the time interval $\tau = t - s$, i.e., $\Delta z_n(s \rightarrow t; -\infty) \equiv z(n, t; -\infty) - z(n, s; -\infty)$. In this case, both $\mathcal{A}_n(\tau)$ and $\mathcal{B}_n(\tau)$ are nonzero with the latter carrying the information of past history of the system and noise, see Eq. (11), and there is no correlation between them. From Eq. (12), the mean square displacement is given by

$$\langle \Delta z_n(\tau)^2 \rangle_s \equiv \langle \Delta z_n^2 \rangle(s \rightarrow t; -\infty) = \langle \mathcal{A}_n(\tau)^2 \rangle + \langle \mathcal{B}_n(\tau)^2 \rangle \quad (46)$$

This is just a repetition of Eq. (45), since the considered situation is precisely the same for the Rouse polymer in thermal equilibrium.

In the transient scenario in equilibrium dynamics, the system starts from the flat interface $z(n, 0) = 0$ for all n , and we monitor the height increment $\Delta z_n(0 \rightarrow t; 0) \equiv z(n, t; 0) - z(n, 0; 0)$, see Eq. (7), where we set $s = T_\infty = 0$, $\tau = t$. In this relaxation process toward equilibrium, $\mathcal{B}_n(\tau) = 0$, hence, from Eq. (12), the mean square displacement is given by

$$\langle \Delta z_n(\tau)^2 \rangle_t \equiv \langle \Delta z_n^2 \rangle(0 \rightarrow t; 0) = \langle \mathcal{A}_n(\tau)^2 \rangle \quad (47)$$

Comparing Eqs (46) and (47), we conclude $\langle \Delta z_n(\tau)^2 \rangle_t < \langle \Delta z_n(\tau)^2 \rangle_s$ due to the lack of $\mathcal{B}_n(\tau)$ factor in the transient result. Indeed, using Eq. (13), we find $\langle \Delta z_n(\tau)^2 \rangle_t = \frac{k_B T}{\gamma} \sqrt{\frac{\tau_0}{\pi}} \sqrt{2\tau}$. Therefore, while $\langle \Delta z_n(\tau)^2 \rangle_s$ and $\langle \Delta z_n(\tau)^2 \rangle_t$ exhibit the same scaling $\sim \tau^{1/2}$, the latter is quantitatively smaller by a factor of $\sqrt{2}$.

Finally, we point out that the above relation between steady-state and transient mobilities in equilibrium dynamics is completely altered in the active dynamics. Indeed, we have demonstrated in the present paper (summarized in Fig. 5 in the main text) that (i) the active systems exhibit different scalings for mean square displacement in steady-state and transient process, (ii) their magnitude relation is $\langle \Delta z_n(\tau)^2 \rangle_t > \langle \Delta z_n(\tau)^2 \rangle_s$ that is opposite to that in the equilibrium dynamics. Our physical picture based on a compounding formula suggests that these properties are expected to be generic in the time scale shorter than the active correlation time τ_A .